



Using LiDAR data to map gullies and headwater streams under forest canopy: South Carolina, USA

L. Allan James^{a,*}, Darrell Glen Watson^a, William F. Hansen^b

^a University of South Carolina, Columbia, SC 29208, USA

^b U.S. Forest Service, 4931 Broad River Road, Columbia, SC 29212, USA

Abstract

The southeastern Piedmont of the USA was severely gullied during the early 20th century. A thick canopy established by reforestation in many areas now inhibits the identification or mapping of gullies by aerial photography or other conventional remote sensing methods. An Airborne Laser-Scanning (ALS or LiDAR) mapping mission flown for the U.S. Forest Service in April, 2004 acquired bare-Earth topographic data. This paper tests the ability of the ALS topographic data to identify headwater channels and gullies for two branching gully systems in forested areas and to extract gully morphologic information. Comparisons are made with field traverses using differential GPS and reference cross sections measured by leveling surveys. At the gully network scale, LiDAR data provide accurate maps – the best available – with robust detection of small gullies except where they are narrow or parallel and closely spaced. Errors in mapping channel location and network topological connectivity under forest canopy increase with attempts to identify smaller features such as large rills. The ability of LiDAR data to map gullies and channels in a forested landscape should improve channel-network maps and topological models. At the gully reach scale, attempts to use LiDAR data to extract gully cross-section morphologic information under forest canopy were less successful due to systematic underestimation of gully depths and overestimation of gully top widths. Limited morphologic accuracy of the data set at this scale may be due to low bare-Earth point densities, shadowing of gully bottoms, and filtering of topographic discontinuities during post-processing. The ALS data used in this study are not suitable for detailed morphometric analysis or subtle change detection to monitor gullies or develop sediment budgets. Data collection may be improved by orienting flights over gullies and with increased point densities through improved scanner technology or better filtering and software capabilities to differentiate between vegetation and ground surfaces.

© 2006 Elsevier B.V. All rights reserved.

Keywords: Gully morphology; Airborne laser scanning; LiDAR mapping; Forest channel networks; Soil erosion; South Carolina Piedmont

1. Introduction

1.1. Importance of ALS mapping

Large gully systems have received much attention from researchers using modern geospatial analysis, especially in the Iberian Peninsula and Africa (Zinck et al., 2001; Martinez-Casanovas, 2003; Martinez-Casanovas et al., 2004). Aerial photography has long been used in gully studies and commercial satellite data have recently become available with the spatial resolutions needed to depict gully development. These methods are less effective in areas covered by heavy foliage, however, especially where abrupt

and frequent surface changes are present. Even in flat areas such as floodplains, the fine details of channel planform are poorly mapped on contour maps of areas under forest canopies. Under closed canopies, channels mapped by interpretations of aerial photographs are often depicted as relatively straight, in conflict with actual channel form and location. A means of generating topographic data in forested areas is needed.

Light Detection And Ranging (LiDAR), *Airborne Laser Scanning* (ALS), or *Airborne LiDAR Swath Mapping* (ALSM) all refer to an active remote sensing technology that can be used to develop high-resolution topographic data over large areas. LiDAR is the most general term and refers to any use of a laser scanner — including oblique land-based systems. ALS and ALSM refer to systems mounted on aircraft and flown over terrain to be mapped. Henceforth, this

* Corresponding author.

E-mail address: Ajames@sc.edu (L.A. James).

paper refers to LiDAR as used for ALS or ALSM. If accurate, LiDAR-derived maps could help identify channel and gully networks, and would improve characterizations of drainage density and fluvial connectivity. These improved capabilities would facilitate topographic, hydrologic, and ecologic modeling.

In addition to improved map precision, accurate LiDAR-derived Digital Elevation Models (DEMs) could be utilized to extract local gully morphologic information for parameterizing runoff, erosion, and sediment transport models. The ability to estimate erosion and sedimentation volumes based on repeated high-resolution topographic data acquisition and standard change-detection procedures would also allow the monitoring of gully morphological changes (Betts and DeRose, 1999). Volumetric assessments of geomorphic change made by differencing sequential DEMs can be used to compute sediment budgets and identify specific sources and sinks of sediment and nutrients (Thoma et al., 2005). Standard DEMs generally lack the spatial and temporal resolution to perform change detection at the local gully scale, but if accurate, ALS data could present the opportunity to monitor hill-slope systems for on-going geomorphic change as is now being done on beaches (Shrestha et al., 2005). LiDAR-generated DEMs would also improve base map information such as slope and drainage density. Digital elevation models (DEMs) have been used to map the development of large gully systems and monitor sidewall erosion or other changes (Betts and DeRose, 1999; Martinez-Casanovas et al., 2004). Creation of accurate, high-resolution DEMs under forest canopy, however, has not been feasible until the recent development of ALS.

This study examines the ability of ALS topographic data to identify, map, and measure the morphology of two gully systems under thick forest canopy in the Piedmont region of South Carolina, USA. Two capabilities of ALS data are assessed: (1) detection and mapping of gully systems under forest canopy, and (2) accuracy of local gully morphological measurements derived from the topographic data. The ability of ALS data to develop accurate maps of gully networks is tested by comparing LiDAR-generated maps with observations in the field. They are also compared with channel networks derived from conventional blue-line and contour-crenulation methods from U.S. Geological Survey (USGS) topographic maps (Strahler, 1957). A second set of tests compares gully morphometric parameters derived from LiDAR-generated DEMs with ground-based topographic surveys of gully cross sections.

1.2. Mapping headwaters and gullies

Accurate identification and mapping of channel headwaters and low-order stream channels is key to physically based characterization of hydrologic processes in small catchments (Tribe, 1990; Wharton, 1994). Headwater streams often account for more than 75% of the length of channels in a basin (Leopold et al., 1964). Moreover, flows

in small channels are often closely linked to nutrient dynamics, macroinvertebrate habitat, and groundwater, so they can be highly vulnerable aquatic ecosystems during dry periods (Meyer and Wallace, 2001; Gomi et al., 2002). Accurate maps of headwater streams are also needed for network analysis to determine drainage densities, stream orders, and stream magnitudes for hydrologic analyses (Melville and Martz, 2004). Because headwaters may be rapidly changed by gullying, a means of on-going monitoring would be quite useful.

Unfortunately, the locations of most headwater streams are not accurately known due to limited resolution of existing maps (Heine et al., 2004). This gap in knowledge extends to fundamental aspects of fluvial systems such as the total length of channels in the United States (Somerville and Pruitt, 2004). The ‘blue-line method’ of delineating channels from maps consistently underestimates the total length of headwater channels (Leopold, 1994). For example, channel lengths derived from blue lines on 1:24,000 U.S. Geological Survey (USGS) quadrangles in the Chattooga catchment of the Blue Ridge Mountains underestimated the extent of intermittent and ephemeral channels and covered only 21% of the total channel length at the 1:24,000 map scale (Hansen, 2001). Blue lines also depend on map scale as was shown in a southern Appalachian Mountains study where the length of channels produced by blue lines ranged from only 0.8 km of channels produced from a 1:500,000 scale map to 56 km from a 1:7200 scale map (Meyer and Wallace, 2001; Somerville and Pruitt, 2004).

1.3. Generating DEMs and channel network maps for small catchments

Topographic modeling techniques applied to DEMs have become standard methods of mapping hydrologic parameters. DEMs can be used to extract channel networks, drainage divides, flow paths, and topologic and morphometric features of catchments that identify processes and facilitate hydrologic modeling of runoff and sediment (Naden, 1992; Beven and Moore, 1993; Garbrecht and Martz, 1993). DEMs can be used to analyze stream order (Lanfear, 1990), drainage patterns (Hadipriono et al., 1990), Hortonian laws of drainage composition and fractal properties of channel networks (Helmlinger et al., 1993; Rodriguez-Iturbe and Rinaldo, 1997), and soil distributions (Klingebiel et al., 1987). The accuracy of derivative products depends on the accuracy and precision of the topographic data used and validation of data to remove erroneous values. The coarse resolution of conventional DEMs (10 × 10 m and 30 × 30 m in the USA) has limited mapping of headwaters and the parameterization of distributed models of small catchments or hill slopes. Verification of headwater locations on channel-network maps is needed because the critical drainage area necessary to initiate channel formation varies between catchments in each region with differences in geology, soils, slopes, vegetation, and land-use histories. To

generate accurate maps of small, headwater channels, high-resolution topographic data are needed.

Several remote sensing methods using traditional classification approaches have been used to delineate large streams and to identify small channels in arid and semi-arid regions where vegetation is sparse (Gardner et al., 1989). The low reflectivity of near-infrared (NIR) radiation by water often allows identification of large water bodies, moist floodplains, wetland soils, and hydrophytic vegetation. The delineation of small channels in vegetated areas has been problematic, however, for digital image classifications and visual interpretations (Wharton, 1994). Similarly, mapping topographic relief under vegetation with aerial photography or satellite imagery can be difficult and inaccurate. Conventional photogrammetric methods lack the ability to penetrate forest canopy. Thus, existing topographic maps of forested areas generally fail to identify geomorphic features at the scale of narrow entrenched channels and gullies (Fig. 1). This paper examines the ability of ALS to produce accurate topographic maps of gully systems under forest canopy in the southeast USA.

1.4. Physiography and erosion in the South Carolina Piedmont, USA

The study area is in the Sumter National Forest (SNF) of the South Carolina Piedmont in the southeastern USA (Fig. 2). The southern Piedmont has a gentle regional slope to the southeast from the Blue Ridge escarpment which lies to the west. The beveled Piedmont surface was not glaciated during the Pleistocene and is dissected with moderate to steep valley side slopes developed in metamorphic or other

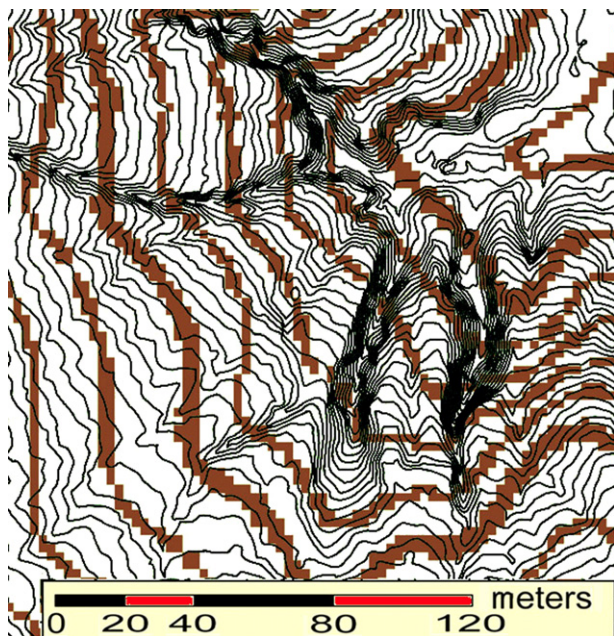


Fig. 1. LiDAR-derived 0.6-m contours (thin lines) superimposed on blow-up of standard USGS 1:24,000 Digital Raster Graphics (DRG) quad 3-m contours (thick blocky lines). Macedonia gully system.

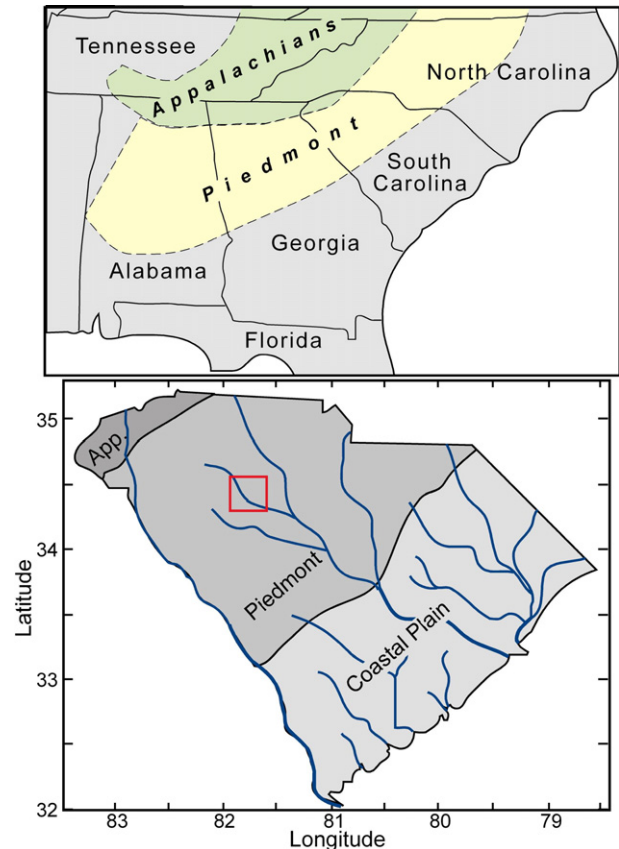


Fig. 2. Study area in the upper Piedmont of South Carolina, USA.

crystalline rocks. Thick forests are often rooted in deeply weathered saprolite that can reach 20 m in depth. To the north in Virginia, similar deep saprolite was described in detail by Pavich (1986) who concluded from an analysis of cosmogenic radionuclides that the weathering front at the base of the saprolite is lowering at a rate that is in equilibrium with landscape down-wearing. He noted that this long-term equilibrium explains the beveled southeast-sloping form of the Piedmont rather than the fluvial planation and peneplain formation postulated by the classic Davisian model. Bulk densities of the metamorphic saprolite below the B horizon are often less than one, but B horizons of the old residual soils are often quite dense with pedogenic clay. This often results in slow initial development of V-shaped gullies but accelerated erosion with wide bases and overhanging root mats once gullies breach the B horizon (Ireland et al., 1939).

The southern Piedmont experienced some of the most severe erosion in the United States due to land clearance by settlement during the nineteenth and early twentieth century. Forest clearance for agriculture and careless tillage practices laid hilly lands bare, and intense rainfalls initiated deep gullying that rendered large areas of farmland useless (Bennett, 1939; Ireland et al., 1939; Trimble, 1974). Many areas of the SNF were logged, farmed repeatedly, and abandoned when erosion and nutrient depletion became so severe that the land could not support cotton or tobacco crops

(Trimble, 1974). Some abandoned lands were later cleared and farmed again and generated a later phase of sheet and gully erosion. Gully erosion developed not only from erosion of agricultural land, but also where artificially concentrated flows breached surface soils to expose the highly erodible saprolite. Some lands were too steep to farm intensively, but road access to remove timber or to provide transportation routes delivered concentrated runoff to erodible soils.

An estimated 200 km² of actively eroding gullies and severely eroded soils initially dissected the Sumter National Forest (SNF) when most of the land was acquired in the early 1930s. The average soil loss from the SNF has been estimated at about 20 to 30 cm of soil, and sediment often filled downstream valleys to depths up to 3 m (Trimble, 1974). By the 1930s, land destruction by gully erosion had reached devastating proportions and soil conservation and erosion research were being initiated. Several gullies in this region were described in a seminal report about Spartanburg County, the adjacent county to the north (Ireland et al., 1939). Other examples of incised channel and gully research were summarized by Schumm et al. (1984). Hoover (1949) described the hydrological changes in soil properties from the cultivation and erosion within the Piedmont including reduced hydraulic conductivity from clogging of the macropores with fine particles and increased runoff response. Bottomland sedimentation in the Piedmont was described by Happ (1945) and Happ et al. (1940).

Many gullies in the southern Piedmont stabilized following the decline of agriculture from the 1940s through 1960s. This period was accompanied by reforestation and successful implementation of soil conservation and rehabilitation measures including erosion-control structures and the introduction of kudzu. Mitigation measures on the SNF involved planting loblolly pine (*Pinus taeda*) across the landscape and treating specific gullies (Hansen, 1991, 1995). Efforts to stabilize gullies varied from internal measures to control headcuts and grade changes such as rock check dams, grade-control structures, and gully plugs. Measures to fill and reshape gullies were used in some instances to help restore the function and capability of the affected area and adjacent lands, rather than just stabilizing the erosion and gully expansion. The assumption is often made that active gully erosion in the region is no longer a serious problem, although recent gully studies are rare. Extremely small gullies contribute runoff and sediment primarily in tropical storm episodes as evidenced by the 48 tonnes delivered by a 0.1 ha discontinuous valley side gully over a 9.5-year period (Hansen and Law, 2006). Some gullies for which the history is known from early surveys (Ireland et al., 1939) have active branches of a relatively young age (Kolomechuk, 2001). Evidence of on-going gully activity – coupled with the generation of non-point source pollution and threats to transportation routes – calls for improved methods of gully monitoring. This study was conducted on two gully systems known as the Macedonia Lake (Mace) and the Compartment 32 (Comp32) gully systems (Fig. 3). Both systems are

located in Union County in the Sumter National Forest, South Carolina and consist of branching networks of multiple gullies.

2. Technical aspects of laser-scanned topographic data

2.1. ALS physical systems and applications

Laser scanners are optical–mechanical devices that actively generate a pulsed laser beam (Wehr and Lohr, 1999). The pulsed scanning laser is coupled with a receiver, an inertial measuring unit that compensates for aircraft motions, a kinematic Global Positioning System (kGPS), and at least one GPS base station to precisely locate the aircraft (Jensen, 2000). The ranging unit of an ALS system measures the time (ns) between emission of the laser beam and receipt of return signals from reflected energy, and converts this time to a distance. The data collected consist of a dense three-dimensional cloud of irregularly spaced points near the Earth's surface. Processing these data can produce a map of *bare-Earth postings* (point elevations of the ground surface with buildings and vegetative canopy removed) that are used to generate high-resolution digital topographic products such as triangulated integrated networks (TINs), DEMs, and contour maps.

The potential of ALS technology is promising for many applications as LiDAR data are becoming commercially available from a variety of vendors, the price of data acquisition and processing is dropping, data resolutions are increasing, and multispectral scanners are under development. ALS can quickly provide topographic maps that are comparable to maps derived photogrammetrically but their ability to penetrate vegetation canopy sets them apart (Balt-savias, 1999a). ALS topographic data have been used to characterize gullies and channels (Ritchie et al., 1994), vegetation cover (Moffiet et al., 2005), beach erosion (Shrestha et al., 2005), landslides (McKean and Roering, 2004; Glenn



Fig. 3. View to ENE up gully F (straight ahead) and gully E (to left) of Mace gully system. Leaf-off condition in February, 2005. This lower position is covered largely by young hardwoods while upper slope has more pine.

et al., 2006), tectonic scarps and glacial fluting (Haugerud et al., 2003), channel-bank erosion (Thoma et al., 2005), floodplain maps for hydraulic modeling (Pereira and Wicherson, 1999), and roughness coefficients for hydraulic modeling (Cobby et al., 2001). In spite of the many successful uses of ALS, limitations of the data for geomorphic purposes have been noted (Kraus and Pfeifer, 1998; Baltsavias, 1999a) and much work is needed to evaluate the accuracy of ALS data for specific applications.

2.2. LiDAR topographic accuracies

Errors in the raw ALS data accumulate from multiple systems including the GPS position, inertial measuring unit orientation, and the laser rangefinder (Baltsavias, 1999b). Outliers may result from scattered energy or complex reflected pathways and are usually removed by pre-screening. The scanners described here collect multiple returns with the first return usually from the top of the canopy and the last return possibly from the bare Earth. Processing to distinguish bare-Earth points from other points is an area of active research and is done by a combination of automatic filtering and manual selection techniques (Petzold et al., 1999; Axelsson, 1999).

Commercially advertised Root Mean Square Errors (RMSE) of LiDAR bare-Earth data typically range from 1 to 2 m in the horizontal and 15 to 20 cm in the vertical dimension, but these measurements are derived where errors tend to be low; that is, on relatively flat areas without discontinuities or thick vegetation. Precision tends to be less near channels due to thick riparian vegetation and steep banks and scarps. LiDAR RMSE in a high-relief area near Green River, Utah was found to be 43 cm due to greater importance of horizontal accuracy in areas of high topographic variability (Bowen and Waltermire, 2002). In the North Carolina Piedmont, the precision of LiDAR bare-Earth elevations was tested with ground surveys under several land covers and types of foliage (Hodgson et al., 2003). The mean vertical LiDAR RMSE was found to be 93 cm; which was less error than IFSAR (X-band radar) data or U.S. Geological Survey Level 1 and Level 2 DEMs. Errors were least in low and high grass (33 and 37 cm), intermediate under pine forest (46 cm), and highest in mixed forest, deciduous forest, and scrub or shrubland (113, 122, and 153 cm, respectively). Thus, vertical errors in bare-Earth maps on the order of one meter are more realistic than RMSE values commonly reported by LiDAR-acquisition companies. Level 2 DEMs produced average RMSE values of 163 cm while Level 1 DEMs had an average RMSE of 743 cm and are not suitable for topographic mapping. The IFSAR data had the greatest RMSE (1067 cm) and systematically overestimated elevations, presumably due to the large size of the IFSAR return beam (Hodgson et al., 2003).

The spatial resolution of laser scanner return data constrain the accuracy of large-scale mapping. Spatial

resolutions can be measured by mean point densities or mean point spacings. As the density of bare-Earth points decreases, the ability of filters to distinguish between vegetation or objects and the ground surface decreases, although this source of error may be less than errors associated with complex surfaces such as steep or vegetated slopes and discontinuities (Sithole and Vosselman, 2004).

3. Methods and data

The ALS data used in this study were collected by Ayers and Associates, Atlanta, Georgia, USA, by fixed-wing aircraft in April, 2004 for the U.S. Forest Service (USFS), Enoree Ranger District. The LiDAR point data were filtered by Ayers and Associates to select bare-Earth estimates which were provided to the USFS in ASCII text files as *X*, *Y*, *Z* values with state plane coordinates. The postings were converted to shapefiles and reprojected into UTM coordinates using ArcGIS 9.0 and most of the raster processing was done using Arc Hydro[®] within ArcGIS Spatial Analyst (ESRI Corp.). Average bare-Earth point densities were 955 points/ha for the Comp32 system and 1275 points/ha for the Mace System (Table 1). The average point spacing is on the order of 3.0 m. Lower point densities for the Comp32 data set may indicate a higher proportion of point removal by filtering, possibly due to points eliminated from steep sidewalls and kudzu-covered gully heads on that system.

The LiDAR bare-Earth point data were used to generate a TIN for each of the two gully systems and three DEMs were generated from the TINs. Two DEMs were generated for the Mace system, at 2 × 2-m and 4 × 4-m grid-cell spacings, and a 4 × 4-m gridded DEM was generated for the Comp32 system. Contour maps were generated from the 4 × 4 DEMs for qualitative field evaluations and for deriving gully networks by the contour crenulation method. Flow lines, accumulation values, stream orders, stream magnitudes, and drainage divides were determined using the hydrologic tools of Spatial Analyst. Five channel networks were derived for each of the two gully systems: the blue line method, crenulations on USGS 1:24,000 contour maps, crenulations on contours from LiDAR-derived 4 × 4-m DEMs, and by automatic raster GIS processing at two accumulation thresholds. The blue line method of delineating channels from blue lines on maps and the crenulation method of delineating channels from shapes of contours are described by Morisawa (1957). Thresholds of accumulation to define the drainage area at which channels were initiated were set at 50 grid cells (800 m²) for one set of

Table 1
LiDAR statistics

| | Bare Earth points | Drainage area | Point density | Point spacing | |
|--------|----------------------|------------------|------------------|--------------------|------|
| | <i>N</i> | ha | Pts/ha | Pts/m ² | |
| Mace | 8939 | 7.01 | 1275 | 0.13 | 2.80 |
| Comp32 | 11,972 | 12.54 | 955 | 0.10 | 3.24 |

networks and 100 grid cells (1600 m²) for the other. Selection of these two threshold values was assisted by comparisons of the resulting channel networks with the LiDAR-generated contour maps to identify a drainage density representative of the dissected landscape. Based on 1:24,000 contour maps, much higher thresholds would have been selected and lower drainage densities would have resulted. Strahler stream orders and Shreve magnitudes (Strahler, 1957; Shreve, 1965) were generated for each network using Spatial Analyst hydrologic tools.

In addition to LiDAR data, two types of ground-truth data were collected in the field during spring and summer of 2005. GPS points were collected in both gully systems along selected gully rims and thalwegs and at cross-section end points. GPS points were collected with a mapping-grade Trimble Pro XR 12-channel differential receiver and differentially corrected using a permanent base station. This system is capable of producing sub-meter horizontal and vertical accuracies under cropland (Trimble Navigation, 1998), although forest canopy and distance to the base station presumably reduced precision. For the morphological evaluation of LiDAR DEMs, conventional leveling was used to survey 14 gully cross sections in the Comp32 system and 23 cross sections in the Mace system. Gully cross-section field transects were compared with cross sections at the same sites extracted from the LiDAR DEMs using *Profile Extractor*, an extension to ESRI ArcView 3.3. The *x–z* coordinates were extracted along transects defined by GPS coordinates of the field cross-section survey endpoints. *Profile Extractor* can be applied in two interpolation modes: the default mode smooths increments between points and the gridded mode produces stair-stepped profiles. Cross-section data were generated in both modes on a few trials, but smoothing was found to remove local steps with horizontal spacings on the order of 30 cm that had no effect on the overall shape of the cross sections, so the default mode of smoothing was used for the LiDAR sections. The resulting gully cross-sections derived from the DEM were visually compared with the ground surveys by overlying plots derived by both methods. Drainage densities for each gully network were computed from total channel lengths taken from GIS attribute tables and dividing them by the drainage area of the gully system which was held constant for all networks of a given system. The accuracy of LiDAR-generated divides and drainage areas was not formally tested but the maps of catchments were far superior to those delineated from the contours on 1:24,000 USGS quadrangles or from available USGS 30-m DEMs.

4. Results and analyses

4.1. Maps of gullies and headwater streams

The ALS data produced topographic maps that are far superior to existing 1:24,000 topographic maps including areas mapped under thick forest canopy. The maps reveal

topographic features beneath the forest canopy that are not depicted on existing maps or aerial photographs, and would otherwise go undetected. For example, agricultural terraces under pine forest that were installed almost 50 years ago as part of a gully rehabilitation project are detected as regularly spaced contour lines (Fig. 4). In the Mace and Comp32 gully systems, forest thinning has generated a uniform spacing of the pine trees with a thick layer of pine needles and little understory vegetation. Reconnaissance mapping with GPS surveys indicates that the LiDAR-generated gully network maps are planimetrically accurate within a few meters which is sufficient for many land-resources management and hydrologic applications. GPS points collected along gully rims

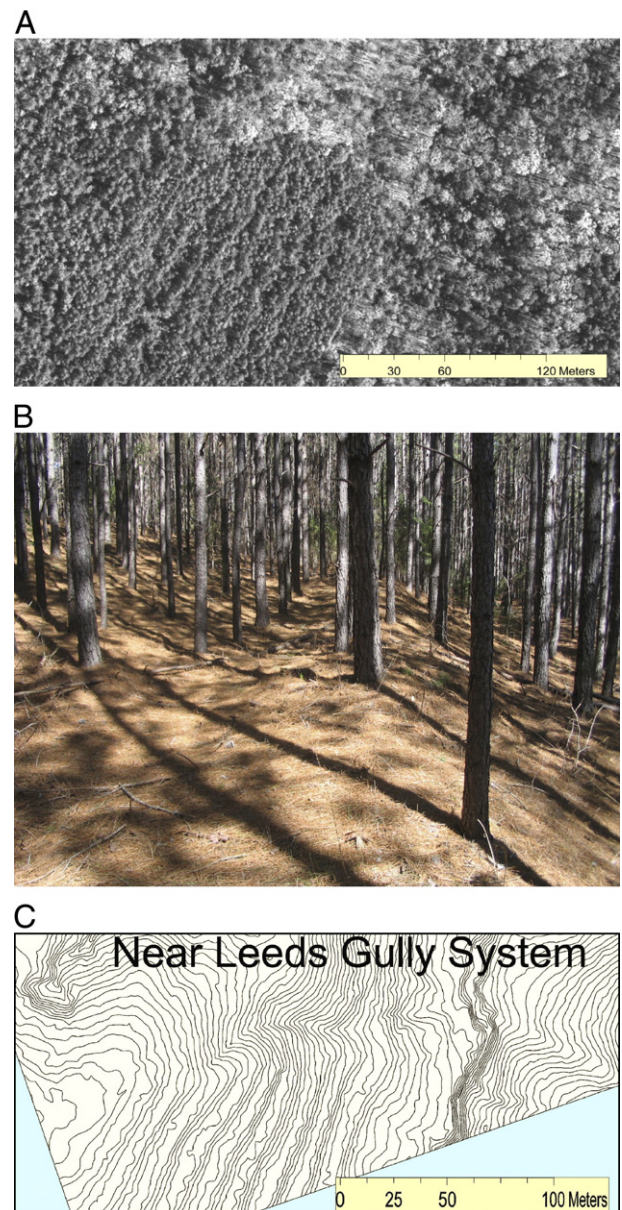


Fig. 4. Terraces beneath pine forest show up as a distinct pattern. (A) Digital Orthophoto Quad (DOQ) showing lineations at pine plantation in southwest corner. (B) terracing on forest floor. (C) LiDAR-derived contours at 0.6-m intervals showing distinctive topographic expression of terracing.

and thalwegs overlay accurately onto LiDAR-generated contour maps and delineate individual gully branches at the scale of the branching systems. Morphologic discrepancies emerge as maps are enlarged to the scale of individual cross sections, and this is addressed in the next section on gully cross-section morphology.

The LiDAR maps of gullies are most distinct for wide, deep gully systems with steep headwalls. These tend to be older gullies that have deepened then widened. Gullies that have not penetrated to saprolite are often relatively narrow, shallow, and V-shaped and can be more difficult to detect, especially in their upper reaches. The two gully systems examined are quite distinct in this respect. Comp32 is developed in less steep terrain and consists primarily of deep, wide gullies with bulbous headwalls that form a dendritic network of limited extent with few upland channels (Fig. 5A). A partially preserved mid-gully terrace indicates that this system was formerly a relatively wide, shallow hollow that was incised and extended by historical erosion. These deep, wide gullies are easily detected and mapped. In contrast, the Mace system is developed on steeper hill slopes and is dominated by long, shallow, V-shaped gullies that form a radial drainage pattern reflecting the basin shape (Fig. 5B). The ALS data had difficulty distinguishing some small parallel gullies and this resulted in errors of omission. The clear detection of parallel stabilization terraces (Fig. 4) suggests that the limitation is not due simply to parallelism but also arises from other factors discussed later. Channel networks generated from LiDAR-derived topographic data reveal substantial improvements in detail over networks derived from alternative data. The resulting networks are relatively accurate for large gullies but are over-simplified in some cases — particularly in the Mace gully system where adjacent small gullies were combined into single channels (Fig. 5). Even with such errors, however, the resulting maps of gully systems under canopy are far superior in resolution and accuracy to alternative maps derived from conventional remote sensing data.

As expected, the blue-line method of delineation underestimated all values of drainage network development and hydrologic connectivity. No blue-line channels are depicted in the Mace catchment and only one first-order channel 140 m long is shown for the Comp32 system (Table 2). Thus, blue-line drainage densities of the two systems are extremely low (zero and 11 m/ha, respectively). Using the contour-crenulation method on 1:24,000 topographic maps produced a substantial improvement over the blue line network maps by indicating 3rd-order networks for both the Mace and Comp32 systems and more realistic drainage densities. Some of the crenulation ‘channels’ appear merely as undulations in the topography and would be difficult to distinguish as active channels without field visits. While the undulations in the two study catchments are known to be occupied by gullies, in otherwise similar areas they have no channels or have gullies that have healed after years of forest recovery and no longer carry concentrated flows in response to storm events.

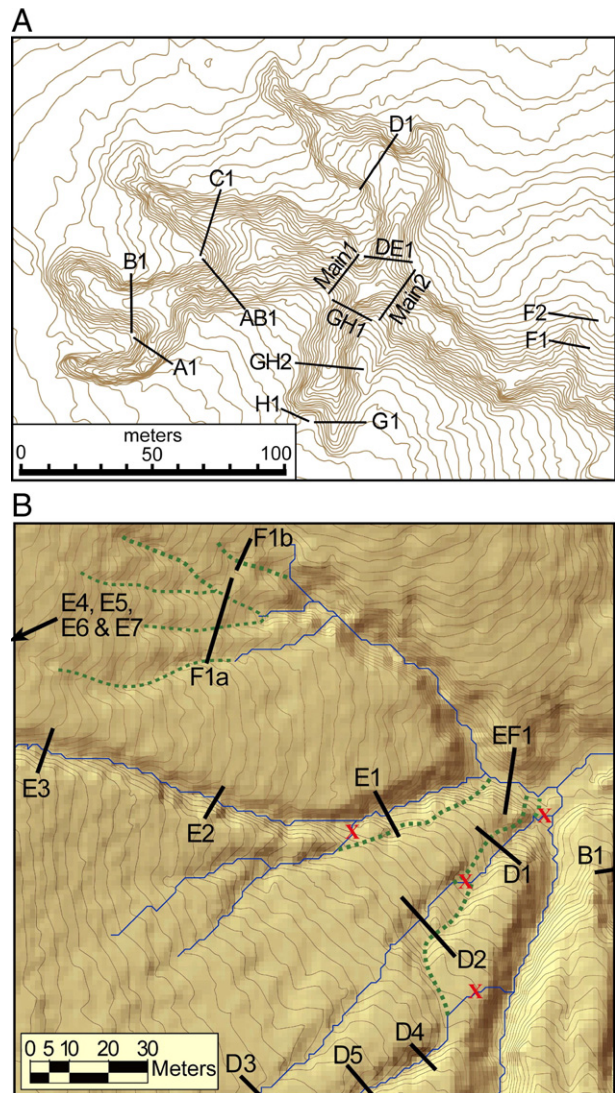


Fig. 5. Contour maps generated from LiDAR-derived 4×4-m DEMs with field-surveyed cross-section locations. Contour intervals are 0.6 m. (A) Comp32 gully system. (B) Mace gully system with topologic errors (X's) and omitted channels (dashed) where small parallel gullies were not detected (see text for explanation).

The gully network maps that best represent field observations are those developed by applying the contour-crenulation method to contour maps generated from the LiDAR-derived DEMs. This method of mapping channels from the shapes of contour lines was assisted by knowledge of the sites obtained during field surveys, but the channels mapped were clearly demarcated by contours and little ambiguity attended the mapping process. Some small gullies and several large rills are not depicted by contour crenulations and are not included on these network maps which are, therefore, a conservative estimate of concentrated flow lines on these slopes. The resulting maps produced 4th and 3rd order streams, and 19 and 14 magnitude streams for the Mace and Comp32 systems, respectively (Table 2). Drainage densities of the networks produced in this way

Table 2
Gully statistics derived from GIS analysis

| Network mapping method | Order (Strahler) | Magnitude (Shreve) | Total length (m) | Drainage density (m/ha) | Comments |
|---------------------------|------------------|--------------------|------------------|-------------------------|-----------------------------|
| Macedonia Lake | | | | | |
| Threshold 50 (Arc Hydro) | 4 | 20 | 1988 | 284 | Threshold=50 grid cells |
| Threshold 100 (Arc Hydro) | 3 | 12 | 1453 | 207 | Threshold=100 grid cells |
| Contour crenulation 4×4 | 4 | 19 | 2451 | 350 | Using LiDAR-derived DEM |
| Contour crenulation Quad | 3 | 5 | 798 | 114 | Using USGS 1:24,000 map |
| Blue line | 0 | 0 | 0 | 0 | 1:24,000 Philson Quadrangle |
| Compartment 32 | | | | | |
| Threshold 50 (Arc Hydro) | 4 | 47 | 3372 | 269 | Threshold=50 grid cells |
| Threshold 100 (Arc Hydro) | 3 | 24 | 2609 | 208 | Threshold=100 grid cells |
| Contour crenulation 4×4 | 3 | 14 | 1154 | 92 | Using LiDAR-derived DEM |
| Contour crenulation Quad | 3 | 6 | 895 | 71 | Using USGS 1:24,000 map |
| Blue line | 1 | 1 | 140 | 11 | 1:24,000 Sedalia Quad |

were much greater than those computed from the 1:24,000 quadrangle maps and differed greatly between the two gully systems. The Mace system is steeper and more dissected than the Comp32 system.

Reasonably good gully networks were also produced automatically by applying the hydrology modules of Spatial Analyst within the ArcMap GIS software to the 4×4-m LiDAR-derived DEMs. The two iterations run on each gully system based on accumulation thresholds of 50 and 100 grid-cells produced similar networks with varying drainage densities. The threshold method is based on a critical drainage area for channel initiation, so the networks based on a 50-cell threshold resulted in similar drainage densities in both basins (~275 m/ha) and the 100-cell threshold networks had lower densities (~207 m/ha). In the Mace system, the 50-cell threshold more closely emulated the drainage density of the preferred contour crenulation method (350 m/ha), although it overestimated channel lengths on broad upland convex slopes and underestimated the density of channels on steeper mid-slope areas. In the Comp32 system, both thresholds overestimated the crenulation drainage densities by mapping extensive channels on uplands where little concentrated flow is now occurring. These contrasts between networks on the two nearby drainage systems illustrate the need for independent calibration of channel network models and suggest that combining slope gradients with critical drainage areas could improve automated drainage network computations at this scale.

4.2. Extracting cross-section morphological information

At the cross-section scale, the morphology of gullies was poorly represented by the ALS topographic data due to consistent underestimation of gully depths and overestimation of top widths (Figs. 6 and 7). The profile sections extracted from LiDAR-derived DEMs fail to accurately characterize the deep, steep-walled gully sections but are shallow and rounded off at the rims as if they were much older and stable than they actually are. In the Mace system, where long but small parallel gullies are separated by less than 10 m, the extracted profiles often failed to distinguish

between the two gullies and produced a single shallow, wide channel. This merging of channels explains the inability of the flow accumulation model to delineate an accurate network at these locations. The LiDAR-derived contour map (Fig. 6B) also fails to clearly distinguish two channels in some places suggesting that the problem is inherent to the DEM and is not simply a problem with Profile Extractor. In addition, the bare-Earth point data in this and other locations show a non-random point distribution aligned with the gullies suggesting a biased filtration of data (Fig. 8).

Point spacings of the LiDAR data used in this study are approximately 3.0 m which supports the generation of 4×4-m DEMs. Theoretically, the Nyquist frequency (twice the grid-cell size) represents the minimum size of topographic features that can be delineated by a grid-based DEM (Warren et al., 2004). By this theory, the data should be able to resolve geomorphic features no smaller than 8 m. Many of the gullies detected in this study have top widths less than 5 m, but as expected, their morphology is poorly represented. Given mean point spacings less than 4 m, a 2×2-m DEM was generated from the original LiDAR data for the Mace system in an attempt to improve the gully cross-section morphology. Cross sections generated from the 2×2-m DEM using Profile Extractor were indistinguishable from those generated from the 4×4-m DEM and provided no improvement. This indicates that additional information about the cross-section shape cannot be extracted from the existing point data simply by increasing DEM resolution.

The bias towards wider and shallower depictions of deep, narrow gully systems limits the ability of these data to identify erosion-prone zones or to detect changes through time. Standard GIS procedures can identify slopes between adjacent grid cells and produce grid maps that suggest locations of likely erosion. GIS-derived slope maps are commonly used as inputs to hill-slope erosion models. However, the accuracy of these procedures depends on the precision and resolution of the DEMs. The systematic underestimation of cross-section side slopes produces unrealistic slope maps within the gullies. Nor is it feasible at this level to use these maps to monitor change or to calculate erosion and sedimentation volumes. Differencing

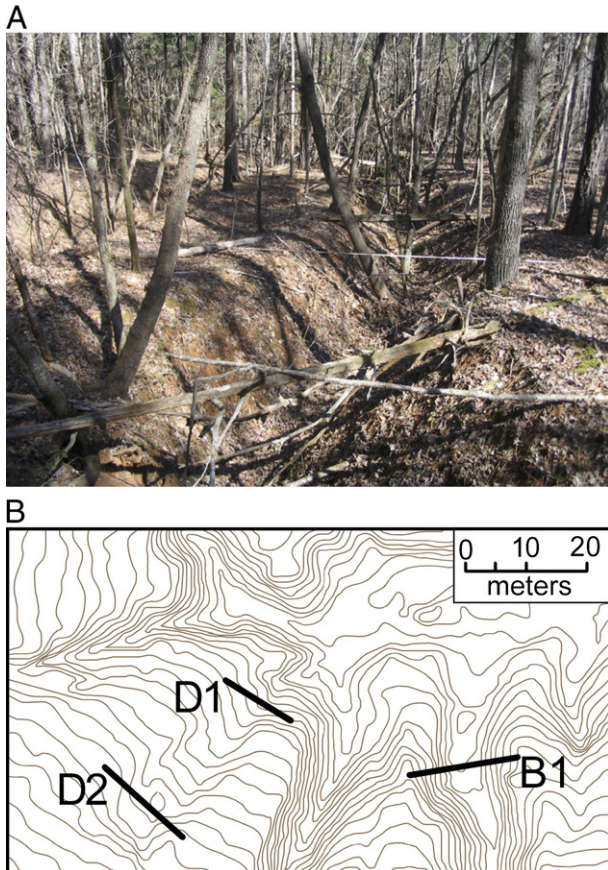


Fig. 6. Two small parallel V-shaped gullies in Mace system. (A) Photograph down center of eastern gully D at section D2 which is ~ 2 m deep at this location. LiDAR-derived data did not detect inter-gully divide on left bank. (B) Map of site with 0.6-m contour interval.

DEMs from sequential ALS flights with the observed accuracies will not likely detect gully changes except where new gully branches are established or substantial enlargement occurs.

5. Discussion

5.1. Possible explanations for morphological limitations

One reason for the underestimates of gully depths and slopes is the limited spatial resolution of bare-Earth data; i.e., point spacings limit the resolution of DEMs derived from the point data. Other factors may also contribute to the limited morphometric precision, such as shadowing of non-vertical laser beams or biased filtering of gully rims. A similar morphometric bias was noted with higher resolution LiDAR data used to map gullies in Germany (Markus Dotterweich, personal communication). The inability of LiDAR-derived DEM data to map the bottoms of deep, steep-walled gully bottoms in that study was attributed to off-nadir angles of laser beams (Fig. 9). If so, positioning of flight lines during ALS data collection more directly over discontinuities could reduce the shadowing effect. In general, ALS data are

collected across a relatively small scan angle between 20 and 40° (Kraus and Pfeifer, 1998), however, so bottom shielding by off-nadir angles should be limited to side slopes greater than 50 to 70 degrees. Many gully slopes are steeper than 60 degrees which may explain the depth underestimations observed in this study. If this factor is important, gully morphology may be measured more accurately at selected sites when scanned from an orientation so that the scanner is directed longitudinally into the gully. This should be a testable hypothesis.

In addition to underestimation of depths, gully top widths were consistently over-estimated. This suggests that many bare-Earth points along gully rims may have been erroneously removed by filtering or manual processing; that is, a Type I error of omission. Filtering may have removed bare-Earth points along rims because they are misinterpreted as vegetation understory or discontinuities caused by objects (beams 3 and 5 in Fig. 9). The point data superimposed on the contour map reveal a tendency for points to be aligned along gully margins suggesting a systematic removal of adjacent points (Fig. 8). Most algorithms remove points near abrupt changes as they are interpreted as objects, so it may be possible to improve accuracies of gully morphometry by adjusting the filtering of returns. The mid-tier canopy is sparse in much of the two gully systems studied, so relaxing

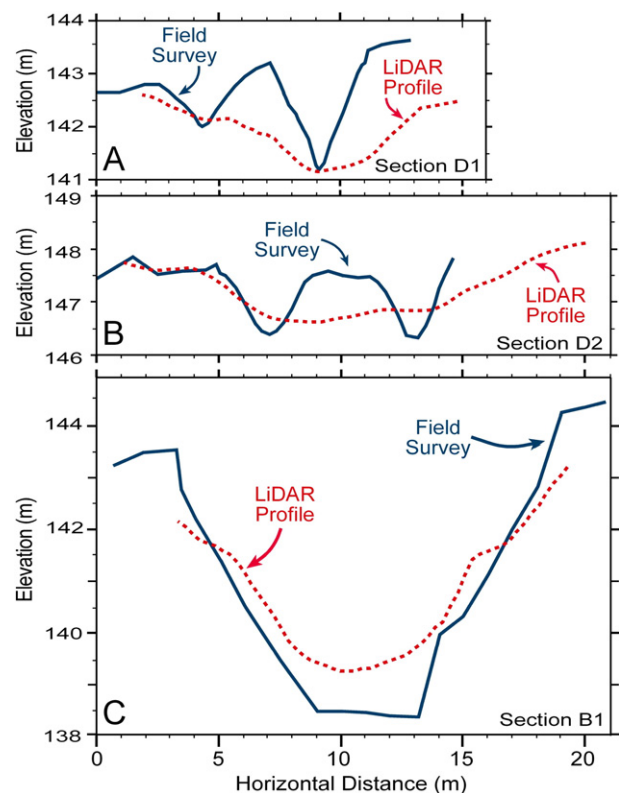


Fig. 7. Comparison of field-surveyed and LiDAR-derived cross sections at two locations across twin gully sites (see Fig. 6 map). (A) Lower profile across two small parallel gullies. LiDAR data fail to distinguish the two gullies. (B) Similar results for same two gullies up-slope at section D2. (C) Profiles in larger single gully; LiDAR underestimates depths and side slopes.

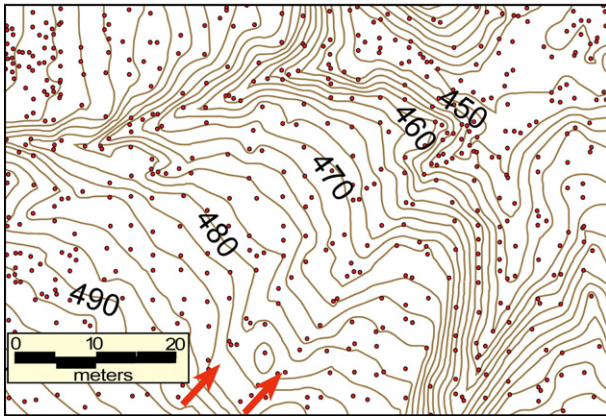


Fig. 8. Portion of LiDAR-derived contour map from Mace system showing bare-Earth data points. Non-random point alignments along and between gullies suggest biased filtering (arrows). Contour interval is 0.6 m; numbers give feet above mean sea level.

filter parameters could improve results. Although the filter algorithms used in this study are proprietary and the details about how these data were filtered are unknown, much can be learned by reviewing basic principles of filter methods.

5.2. ALS data filtering

The ALS point cloud must be filtered to separate points representing canopy and human structures from the bare-Earth points that are used for topographic mapping. This filtering greatly influences the accuracy with which gully morphology is represented in the bare-Earth data, so selection and implementation of an appropriate filtering algorithm should be optimized to retain steep and vegetated slopes with discontinuities. In rural areas, it may not be necessary to filter discontinuities as aggressively as when buildings and other objects are present. The challenge is to filter out points reflected by vegetation (virtual deforestation) without removing points reflected by the unvegetated Earth. Filtering methods use discriminant functions based on discontinuities such as abrupt differences in height, slope, distance to TIN facets, or distance to parameterized surfaces, so abrupt topographic changes tend to be difficult to distinguish from vegetation and are often filtered from the bare-Earth data. Accuracies of bare-Earth maps are best for surfaces that lack outliers, complex objects such as bridges and buildings, thick vegetation, and abrupt discontinuities (Sithole and Vosselman, 2004). Optimizing the filter to minimize Type I errors (erroneous omission of bare-Earth points) should increase the retention of data along gully rims. Although these algorithms may generate more Type II errors (erroneous positive identification of bare-Earth points), those points tend to be fewer in number and have less influence on total error than Type I errors (Sithole and Vosselman, 2004). This should be especially true in rural areas where discontinuities are less likely to be structures. Moreover, Type II errors tend to be conspicuous and are easier to remove manually than Type I errors. The retention of data

along discontinuities is of great relevance to the identification of steep-walled gullies, so slope-based filters that tend to remove discontinuities may not be appropriate for this purpose.

The derivation of DEMs from LiDAR data and calculations of slope from them using standard geospatial processing methods are also associated with error. Common GIS slope-calculation methods can produce variable results depending on algorithms used, preprocessing, DEM resolution, slope gradient, and other factors (Warren et al., 2004; Weih and Mattson, 2004). Slope computation methods often produce errors that are negatively correlated with slope due to overestimation of slope in flat areas and underestimation in steep areas. The best results tend to be obtained from high-resolution DEMs generated by using elevation data from large areas surrounding a given grid cell (Warren et al., 2004).

5.3. Recommendations and future analyses

Application of ALS technology to hill-slope mapping should be promoted as a high priority for land and water resources management purposes and for scientific research. ALS technology can greatly improve channel network maps under forest canopy and topologic analyses such as stream-ordering at levels of precision not previously possible by standard remote sensing methods. If possible, data accuracies should also be improved to enable identification of local geomorphic features that are diagnostic of erosion processes. Gully morphology is closely linked to geomorphic processes, so recognition of the potential for gully enlargement or stabilization should be based, in part, on a careful examination of form within gully systems. For example, monitoring of up-gully migration of plunge pools (knick-points) on gully bottoms may indicate whether measures are needed to protect existing structures, facilities, roads, or hydraulic works. Accurate maps of gully widths, depths, and other topographic details would also help with routine planning activities such as stream protection during timbering or land development (Hansen, 2001). Pollutant prevention practices in the USA, such as *Best Management Practices*

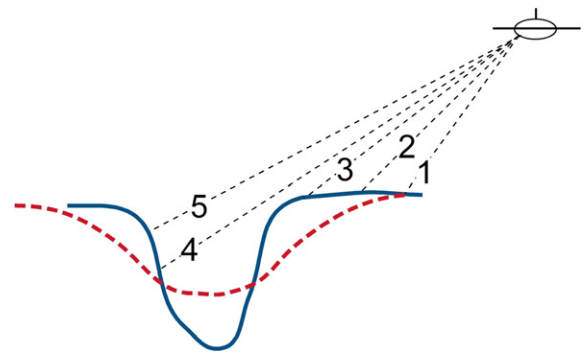


Fig. 9. Hypothetical explanation for filtering of gully rim points from a bare-Earth data set generated by an ALS at an exaggerated low angle. See text for explanation.

(BMPs), require the ability to identify stream types and adjacent slopes and adjust practices within stream-side buffer zones to protect water quality and associated beneficial uses.

Several adjustments to the ALS data collection and processing could improve topographic mapping results. The data used in this study have relatively sparse point densities by current ALS research standards. Average bare-Earth point spacings of approximately 30 cm are now achievable and some systems are capable of even smaller mean spacings. Higher-resolution images can improve the resolution of DEMs and contour maps, and could improve the sensitivity of the topographic data to abrupt changes in slopes at gully margins. For example, improved LiDAR bare-Earth point densities can be obtained by manipulating the timing of data acquisition, such as by flying during the leaf-off period or following fires or timbering. Higher point densities can also be achieved through reducing the laser ‘footprint’ on the ground by lowering flight elevations, decreasing air speed, or using a scanner with a smaller beam divergence, smaller scan angle, or higher pulse frequency (Wehr and Lohr, 1999). Another adjustment that could improve the ability of ALS data to map gully morphology would be to plan flight lines to optimize scan directions along the longitudinal axis of main gullies and channels. Using a helicopter, it could be possible to position the flight to more accurately capture the details of gully morphologic features. In addition, later flights could be used to monitor changes that are desired for interpretations on sediment, stability and change detection.

Spatial processing of the bare-Earth point data may improve the resolution of morphological details. For example, greater use of TIN data structures could reduce rounding errors introduced by extraction of grid structures during the generation of DEMs. Results may also be improved by incorporating into TIN structures ancillary data from GPS transects along primary breaks in slopes such as the rims and bottoms of gullies. Coordinates of such known discontinuities can be used as *breaklines* to train TIN structures to explicitly delineate these features. Field survey or photogrammetric data can be used to delineate breaklines that can be incorporated in the spatial analysis to reduce topological and topographic errors. These procedures may sharpen the definition of discontinuities and complex morphology in the spatial data and could improve gully mapping. Breakline data were collected but were not included in this analysis which is focused on the ability of LiDAR to generate gully maps and morphologic information over broad areas without reliance on field visits.

6. Conclusions

Detailed topographic data can generate a variety of data products for spatial analysis of channel networks and identification of headwater gullies. These products are of growing importance for hydrologic modeling, water quality assessments, ecological monitoring, aquatic restoration projects, and a battery of other environmental management

objectives. Many gullies and channels can be clearly identified, measured, and mapped on aerial photographs in open areas with no vegetation canopy. LiDAR data may not be needed in these locations, although it provides a relatively fast and efficient means for surveying topographic details over large areas even in these ideal circumstances. A major advantage of ALS surveys is that they can be used to locate and map gully systems that lie beneath thick canopy. This mapping capability should be of increasing importance for gully inventories, hydrologic modeling, determining land-use treatments, and estimating soil erosion and sedimentation volumes. As LiDAR technology becomes cheaper and the analysis and products more refined, applications of the technology will expand.

LiDAR-derived data successfully identified and characterized the location, extent, and density of channels in the two gully systems studied. The data provided superior maps at far higher resolutions than standard topographic maps used in the USA (1:24,000), and did so under foliage. The resulting maps were planimetrically accurate at the scale of branching gully systems and far more accurate and complete than those that can be derived under forest cover from other available sources. At the catchment scale, existing topographic maps and 30×30-m DEMs failed to show gullies, tended to underestimate local slopes, and omitted details of gully morphology. In contrast, the ALS data identified gullies down to approximately 3 m top width and generally mapped their locations accurately under forest canopy. The identification of stream headwaters, mapping of drainage networks, and calculation of drainage densities were greatly improved. This capability should allow improved calibrations of flow-accumulation models for the automatic delineation of drainage networks from DEMs and the parameterization of runoff and non-point-source pollution generation models. Although gullies were occasionally omitted from maps – especially when two small gullies were closely spaced – the resulting network topology and drainage density was a major improvement over current topographic maps, even with crenulation analysis.

At the local scale, LiDAR-derived data provided approximate measures of gully cross-section morphology. These cross sections tended to be too wide and shallow with sidewalls less steep than field-measured values. This inaccuracy in small steep-walled gullies under forest canopy is partly attributable to limited spatial resolutions of the bare-Earth point data, but it may also be the result of biased filtering of the ALS data or shadowing of laser beams due to the deeply entrenched gullies. More research is needed to explain this phenomenon and to seek remedies. At present the effect limits the ability to apply ALS data to models of gully geomorphic and hydrologic processes. Furthermore, the ability to monitor gully development by repeat ALS surveys and to measure on-going gully erosion, sediment production and deposition, or to calculate sediment budgets, depends on precise measurements at the reach scale. On a positive note, ALS data-collection and processing

technology is rapidly improving and this should ultimately allow estimates of gully bed slopes, side slopes, and channel morphology beneath forest canopy.

Acknowledgements

We thank the U.S. Forest Service for cooperation, assistance, and the provision of LiDAR data for the Sumter National Forest. Linni Li assisted with field work. Marcus Dotterweich and an anonymous reviewer provided numerous constructive comments in reviews of a draft of this paper.

References

- Axelsson, P., 1999. Processing of laser scanner data — algorithms and applications. *Photogrammetry and Remote Sensing* 54, 68–82.
- Baltsavias, E.P., 1999a. A comparison between photogrammetry and laser scanning. *Photogrammetry and Remote Sensing* 5, 83–94.
- Baltsavias, E.P., 1999b. Airborne laser scanning: basic relations and formulas. *Photogrammetry and Remote Sensing* 54 (2/3), 199–214.
- Bennett, H.H., 1939. *Soil Conservation*. McGraw-Hill Book Co., N.Y. 993 pp.
- Betts, H.D., DeRose, R.C., 1999. Digital elevation models as a tool for monitoring and measuring gully erosion. *International Journal of Applied Earth Observation and Geoinformation* 1 (2), 91–101.
- Beven, K.J., Moore, I.D. (Eds.), 1993. *Terrain Analysis and Distributed Modelling in Hydrology*. J. Wiley & Sons, N.Y., pp. 1–3.
- Bowen, Z.H., Waltermire, R.G., 2002. Evaluation of Light Detection and Ranging (LIDAR) for measuring river corridor topography. *Journal of the American Water Resources Association* 38 (1), 33–41.
- Cobby, D.M., Mason, D.C., Davenport, I.J., 2001. Image processing of airborne scanning laser altimetry data for improved river flood modelling. *Photogrammetry and Remote Sensing* 56, 121–138.
- Garbrecht, J., Martz, L., 1993. Case application of the automated extraction of drainage network and subwatershed characteristics from digital elevation models by DEDNM. In: Lanfear, K., Harlin, J. (Eds.), *Geographic Information Systems and Water Resources Am. Water Resources Assn.*, pp. 221–229.
- Gardner, T.W., Connors, K.F., Hu, H., 1989. Extraction of fluvial networks from SPOT panchromatic data in a low relief, arid basin. *International Journal of Remote Sensing* 10 (11), 1789–1801.
- Glenn, N.F., Streutker, D.R., Chadwick, D.J., Thackray, G.D., Dorsch, S.J., 2006. Analysis of LiDAR-derived topographic information for characterizing and differentiating landslide morphology and activity. *Geomorphology* 73, 131–148.
- Gomi, T., Sidle, R.C., Richardson, J.S., 2002. Understanding processes and downstream linkages of headwater systems. *BioScience* 52 (10), 905–916.
- Hadipriono, F.C., Lyon, J.G., Li, T.W.H., 1990. The development of a knowledge-based expert system for analysis of drainage patterns. *Photogrammetric Engineering and Remote Sensing* 56 (6), 905–909.
- Hansen, W.F., 1991. Land rehabilitation on the Sumter National Forest. In: Fan, S., Kuo, Y. (Eds.), *Proc. Fifth Fed. Interagency Sedimentation Conference*, vol. 1. Fed. Energy Regulatory Comm.: U.S. Govt. Printing Office, Las Vegas, Nevada, pp. 3-110–3-117.
- Hansen, W.F., 1995. Gully treatments. *Proc. Watershed Assessment and Restoration Workshop*, National Advanced Resource Technology Center. USDA Forest Service, Marana, Arizona.
- Hansen, W.F., 2001. Identifying stream types and management implications. *Forestry and Ecology Management* 143 (1–3), 39–46.
- Hansen, W.F., Law, D.L., 2006. Sediment from a small ephemeral gully in South Carolina. In *Proc. Soc. American Foresters National Convention*, Fort Worth, Texas, 2005.
- Happ, S.C., 1945. Sedimentation in South Carolina valleys. *American Journal of Science* 243, 113–126.
- Happ, S.C., Rittenhouse, G., Dobson, G.C., 1940. Some principles of accelerated stream and valley sedimentation. *U.S. Dept. Agriculture, Technical Bulletin*, vol. 633, pp. 22–31.
- Haugerud, R.A., Harding, D.J., Harless, L.L., Weaver, C.S., Sherrod, B.L., 2003. High-resolution LiDAR topography of Puget Lowland, Washington — a bonanza for Earth sciences. *GSA Today* 13 (6), 4–10.
- Heine, R.A., Lant, C.L., Sengupta, R.R., 2004. Development and comparison of approaches for automated mapping of stream channel networks. *Annals of the Association of American Geographers* 94 (3), 477–490.
- Helminger, K.R., Kumar, P., Foufoula-Georgiou, E., 1993. On the use of digital elevation model data for Hortonian and fractal analyses of channel networks. *Water Resources Research* 29 (8), 2599–2613.
- Hodgson, M.E., Jensen, J.R., Schmidt, L., Schill, S., Davis, B., 2003. An evaluation of lidar- and IFSAR-derived digital elevation models in leaf-on conditions with USGS Level 1 and Level 2 DEMs. *Remote Sensing of Environment* 84, 295–308.
- Hoover, M.D., 1949. Hydrological characteristics of South Carolina Piedmont forest soils. *Proceedings of the Soil Science Society*, pp. 353–358.
- Ireland, H.A., Sharpe, C.F.S., Eargle, D.H., 1939. Principles of gully erosion in the Piedmont of South Carolina. *U.S. Dept. Agriculture Tech.*, 633.
- Jensen, J.R., 2000. *Remote Sensing of the Environment: An Earth Resource Perspective*. Prentice Hall, Upper Saddle River, New Jersey.
- Klingebiel, A.A., Horvath, E.H., Moore, D.G., Reybold, W.U., 1987. Use of slope, aspect, and elevation maps derived from digital elevation model data in making soil surveys. *Soil Survey Techniques*; *Soil Science Soc. Amer. Spec. Pub.*, vol. 20, pp. 77–89.
- Kolomechuk, C. 2001. Gully Erosion in Spartanburg County, Southern Piedmont, S.C. Unpub. Masters thesis. Geography Dept., Univ. South Carolina.
- Kraus, K., Pfeifer, N., 1998. Determination of terrain models in wooded areas with airborne laser scanner data. *Photogrammetry and Remote Sensing* 53, 193–203.
- Lanfear, K.J., 1990. A fast algorithm for automatically computing Strahler stream order. *Water Resources Bulletin* 26 (6), 977–979.
- Leopold, L.B., 1994. *A View of the River*. Harvard Univ. Press, Cambridge, Massachusetts.
- Leopold, L.B., Wolman, M.G., Miller, J.P., 1964. *Fluvial Processes in Geomorphology*. W.H. Freeman and Co., S.F.
- Martinez-Casanovas, J.A., 2003. A spatial information technology approach for the mapping and quantification of gully erosion. *Catena* 50, 293–308.
- Martinez-Casanovas, J.A., Ramos, M.C., Poesen, J., 2004. Assessment in sidewall erosion in large gullies using multi-temporal DEMs and logistic regression analysis. *Geomorphology* 58, 305–321.
- McKean, J., Roering, J., 2004. Objective landslide detection and surface morphology mapping using high-resolution airborne laser altimetry. *Geomorphology* 57, 331–351.
- Melville, J.K., Martz, L.W., 2004. A comparison of data sources for manual and automated hydrographical network delineation. *Canadian Water Resources Journal* 29 (4), 267–282.
- Meyer, J.L., Wallace, J.B., 2001. Lost linkages and lotic ecology: rediscovering small streams. In: Press, M.C., Huntly, N.J., Levin, S. (Eds.), *Chapter 14. Ecology: Achievement and Challenge*. Blackwell Science, Oxford, UK.
- Moffiet, T., Mengersen, K., Witte, C., King, R., Denham, R., 2005. Airborne laser scanning: exploratory data analysis indicates potential variables for classification of individual trees or forest stands according to species. *Photogrammetry and Remote Sensing* 59, 289–309.
- Morisawa, M.E., 1957. Accuracy of stream length determinations from topographic maps. *EOS Transactions AGU* 38, 86–88.
- Naden, P.S., 1992. Spatial variability in flood estimation for large catchments: the exploitation of channel network structure. *Hydrological Sciences Bulletin* 37 (1), 53–71.
- Pavich, M.J., 1986. Processes and rates of saprolite production and erosion on a foliated granitic rock of the Virginia Piedmont. In: Colman, S.M.,

- Dethier, D.P. (Eds.), Rates of Chemical Weathering of Rocks and Minerals. Academic Press, Inc., New York, pp. 552–590.
- Pereira, L.M.G., Wicherson, R.J., 1999. Suitability of laser data for deriving geographical information: a case study in the context of management of fluvial zones. *Photogrammetry and Remote Sensing* 54, 105–114.
- Petzold, B., Reiss, P., Stossel, W., 1999. Laser scanning-surveying and mapping agencies are using a new technique for the derivation of digital terrain models. *Photogrammetry and Remote Sensing* 54, 95–104.
- Ritchie, J.C., Grissinger, E.H., Murphey, J.B., Garbrecht, J.D., 1994. Measuring channel and gully cross-sections with an airborne laser altimeter. *Hydrological Processes* 8, 237–243.
- Rodriguez-Iturbe, I., Rinaldo, A., 1997. Fractal River Basins: Chance and Self-Organization. Cambridge Univ. Press, Cambridge, U.K.
- Schumm, S.A., Harvey, M.D., Watson, C.C., 1984. Incised Channels, Morphology, Dynamics and Control. Water Resources Publications, Littleton, CO.
- Shrestha, R.L., Carter, W.E., Sartori, M., Luzum, B.J., Slatton, K.C., 2005. Airborne laser swath mapping: quantifying changes in sandy beaches over time scales of weeks to years. *ISPRS Journal Photogrammetry and Remote Sensing* 59, 222–232.
- Shreve, R.L., 1965. Statistical law of stream numbers. Publication, vol. 274. Institute of Geophysics and Planetary Physics, Univ. of Calif., Los Angeles, CA, pp. 17–37.
- Sithole, G., Vosselman, G., 2004. Experimental comparison of filter algorithms for bare-Earth extraction from airborne laser scanning point clouds. *Photogrammetry and Remote Sensing* 59, 85–101.
- Somerville, D.E., Pruitt, B.A., 2004. Draft Physical Stream Assessment: A Review of Selected Protocols. Prepared for the U.S. Environmental Protection Agency, Office of Wetlands, Oceans, and Watersheds, Wetlands Division (Order No. 3W-0503-NATX). EPA, Wash., D.C.
- Strahler, A.N., 1957. Quantitative analysis of watershed geomorphology. *Transactions of the American Geophysical Union* 38 (6), 913–920.
- Thoma, D.P., Gupta, S.C., Bauer, M.E., Kirchoff, C.E., 2005. Airborne laser scanning for riverbank erosion assessment. *Remote Sensing of Environment* 95, 493–501.
- Tribe, A., 1990. Automated recognition of valley heads from digital elevation models. *Earth Surface Processes and Landforms* 16, 33–49.
- Trimble, S.W., 1974. Man-Induced Soil Erosion on the Southern Piedmont 1700–1970. Soil Conservation Society of America.
- Trimble Navigation, 1998. Pro XR/XRS Receiver Manual. Trimble Navigation Ltd., Sunnyvale, California.
- Warren, S.D., Hohmann, M.G., Auerswald, K., Mitasova, H., 2004. An evaluation of methods to determine slope using digital elevation data. *Catena* 58, 215–233.
- Wehr, A., Lohr, U., 1999. Airborne laser scanning — an introduction and overview. *Photogrammetry and Remote Sensing* 54, 68–82.
- Wei, R.C., Mattson, T.L., 2004. Modeling slope in a geographic information system. *Journal of the Arkansas Academy of Science* 58, 100–108.
- Wharton, G., 1994. Progress in the use of drainage network indices for rainfall-runoff modelling and runoff prediction. *Progress in Physical Geography* 18 (4), 539–557.
- Zinck, J.A., Lopez, J., Metternicht, G.I., Shrestha, D.P., Vasquez-Selem, L., 2001. Mapping and modeling mass movements and gullies in mountainous areas using remote sensing and GIS techniques. *International Journal of Applied Earth Observation and Geoinformation* 3 (1), 43–53.